# Time Scales and Variability of Area-Averaged Tropical Oceanic Rainfall

KYUNG-SUP SHIN*, GERALD R. NORTH AND YOO-SHIN AHN

*Climate System Research Program, Department of Meteorology, Texas A&M University, College Station, Texas*

PHILLIP A. ARKIN

*Climate Analysis Center, National Meteorological Center, National Weather Service, NOAA, Washington, DC*

(Manuscript received 26 July 1989, in final form 17 January 1990)

ABSTRACT

A statistical analysis of time series of area-averaged rainfall over the oceans has been conducted around the diurnal time scale. The results of our analysis can be applied directly to the problem of establishing the magnitude of expected errors to be incurred in the estimation of monthly area-averaged rain rates from low orbiting satellites. Such statistics as the mean, standard deviation, integral time scale of background red noise and spectral analyses were performed on time series of the GOES Precipitation Index (GPI) taken at 3-hour intervals during the period spanning 19 December 1987 to 31 March 1988 over the central and eastern tropical Pacific. The analyses have been conducted on 2.5° × 2.5° and 5° × 5° grid boxes, separately.

The ratio of standard deviation to mean for area-averaged rain rate in the Pacific ITCZ is very regular and similar to that in GATE. Analysis of the area-averaged rainfall in the SPCZ shows a longer autocorrelation time scale than that in the ITCZ. The SPCZ exhibits significant power at the diurnal and semidiurnal frequencies, but the ITCZ shows only a marginally significant diurnal cycle in our data. The rainfall characteristics in the Pacific ITCZ appear to be similar to those in the Atlantic ITCZ in both autocorrelation time scale and diurnal variation. The mechanism driving convection in the ITCZ is suggested to be different from that in the SPCZ. The study shows that rainfall measurements by a sun-synchroneous satellite visiting a spot twice per day will include a bias due to the existence of the semidiurnal cycle in the SPCZ ranging from 5 to 10 percentage points. The bias in the ITCZ may be of the order of 5 percentage points.

## 1. Introduction

The area–time averaged rainrates in the tropics are a measure of latent heat release, which is vital in the study of the general circulation and short-term climate change. However, due to the large fraction of earth covered by ocean and lack of a proper data acquisition system over the ocean, tropical precipitation data over the oceans are notoriously poor. The obvious solution is to rely on the measurements from space platforms. But measurements from low-earth orbiting satellites produce different types of problems due to the discontinuous nature of the sampling process from such devices.

Sampling errors arise from taking discrete observations in time or in space. Because of the high variability of rainfields in both space and time, discrete observations will contribute to error variance in estimating average rainfall. Raingage measurements give observations continuous in time but discrete in space. The accuracy of estimating average rainfall over an area for a given duration depends on how well the records at the sites of the raingages represent those in between, i.e., the spatial variance of rain rates at small scales. On the other hand, satellite measurements provide observations continuous in space but discrete in time. The accuracy depends on how well the snapshots at the time of measurement represent those in between, i.e., the temporal variance of area-averaged rain rates at small scales.

The sampling-error problem has recently been reviewed by North (1987) and investigated directly with data by McConnell and North (1987), and with stochastic models tuned to data by Bell (1987), Shin and North (1988), Bell et al. (1990) and others. North and Nakamoto (1989) proposed a spectral formalism of sampling error estimation. They showed that the mean squared error could be written as the integral of a product of a design-dependent-filter multiplied by the space-time spectrum of the rainfield. Moreover, they proved that the error structure depends only upon the second moment characteristics of the rain fields. Progress in delineating the error structure of various satellite-observing system designs is being hampered by a lack of

* Present affiliation: Korea Meteorological Service, Seoul, Korea.

*Corresponding author address:* Dr. Gerald R. North, Climate System Research Program, Texas A&M University, College of Geosciences, College Station, TX 77843-3146.

real, dispersed measurements (ground truth) of precipitation data over the oceans. The parameter values that have been used in the studies so far rely too heavily on the GATE rainfall statistics even though the representativeness of the temporal and spatial statistics in GATE throughout the tropical oceans in still in question. This paper attempts to partially remedy this problem.

North and Nakamoto (1989) emphasize the importance of the following factors contributing to large sampling errors for space–time average rain estimates: 1) errors are proportional to the square root of the power spectrum value at the sampling frequency of the observing system. The power spectrum may consist of a red noise background and/or harmonics of the diurnal cycle. Small red noise contribution at the sampling frequency means the autocorrelation time for the area-averaged rain is long. Errors tend to be inversely proportional to the square root of this autocorrelation time; 2) errors are proportional to the standard deviation of the area-averaged rain rate.

For a sun-synchronous satellite, which has two observations per day at 12 h intervals in the tropics, the existence of a semidiurnal cycle will lead to a biased estimate of rainfall, although the diurnal cycle does not contribute to error because of cancelation of the sinusoidal amplitude when sampled at half-periods. If the satellite only returns to the spot once per day, the amplitude of the diurnal sinusoid will be the dominant factor. In fact, a typical sun-synchronous satellite with a microwave radiometer such as the SSM/I on the DMSP satellite returns to an averaging box in the tropics twice per day only about one-third of the days, one-third of the days it passes the spot only once and one-third of the days it misses the spot altogether. The TRMM satellite, whose orbit plane is inclined at 35 degrees with respect to the equatorial plane, returns to a given averaging box at least twice (almost) every day with a revisit interval of 11.75 h, just off the semidiurnal cycle. This latter allows the satellite to sample through the local hours of the day over the course of a few weeks. In the spectral formalism, the sampling frequency just "misses" the semidiurnal cycle.

The diurnal characteristics of tropical rainfall over oceans have been previously investigated for various purposes using many different data sources. For example: Gary and Jacobson (1977) used data taken on atolls or small islands; McGarry and Reed (1978) used shipboard measurements; Gruber (1976), Murakami (1979), Reed and Jaffe (1981), Gruber and Chen (1988), Wexler (1983), and Albright et al. (1985) used outgoing longwave radiation (OLR); and Meisner and Arkin (1987) used estimated rainfall from the GOES precipitation index (GPI). Their results suggest that cycles at the diurnal time scale strongly depend upon geography and season. Albright et al. (1985) presented evidence that a second harmonic is often appreciable over vast regions of the Pacific.

The objective of this study is to investigate the representativeness of GATE rainfall statistics throughout the tropical oceans, especially the ITCZ. In the absence of real rainfall measurements over tropical oceans, the GOES infrared data are utilized as an indicator of rain. Our strategy is to compare statistics of satellite data in different locations with the hope of providing some qualitative evidence to answer the representativeness question. We focus on parameters related to sampling problems of area-averaged rainfall such as the coefficient of variation, the variance at the diurnal and semidiurnal cycles of area-averaged rainfall and the time scale of background red noise. Each of these is examined across the Pacific for both 2.5° × 2.5° and 5° × 5° averaging boxes. Each of these is important in sampling error estimation and bias correction considerations that can be expected for precipitation measurements from low-orbiting satellites.

## 2. Data

In the absence of conventional raingage measurements our only method of estimating rainrate over the world oceans is the indrect method from infrared cloud top temperature from geostationary satellites (Arkin 1979; Richards and Arkin 1981). The GOES-West infrared cloud top temperatures were used in this study. The NOAA/Climate Analysis Center specially archived the data by classifying the brightness temperatures into a histogram of 16 classes (see Meisner and Arkin 1987) for every 2.5° × 2.5° grid box. The data were recorded at 3-hour intervals during 19 December 1987 to 31 March 1988 over the central and eastern tropical Pacific in the area bounded from 20°N to 20°S and from 175°E to 85°W. From the histogram, the GOES Precipitation Index (GPI) was calculated as the ratio of the number of pixels colder than 235 K to the total number of pixels in each 2.5° × 2.5° grid box. The GPI used in this study is basically the same (proportional) as used by Arkin (1983). The GPI for 5° × 5° grid boxes was also calculated by combining the histograms of four adjacent grid boxes. Hereafter the datasets at the different grid resolutions will be referred to as G25 and G50 for the 2.5 and 5.0 grid boxes, respectively, and GPI25 and GPI50 for the GPI of the corresponding area.

The data have some gaps. If data gaps are longer than 12 h, we disregard the entire day of observations and continue the time series with the following day. Otherwise, gaps are linearly interpolated from the time series. Observations from three days were discarded due to long gaps, and interpolated data were about 5% of the total time series. The exclusion of data for an entire day and recomposition may produce artificial statistics in the analysis. However, we have concluded that the effect on our analysis is negligible.

Figure 1 shows examples of the GPI25 time series along the latitude belt lying between 12.5° and 15.0°S. From the top to bottom and left to right in Fig. 1, each

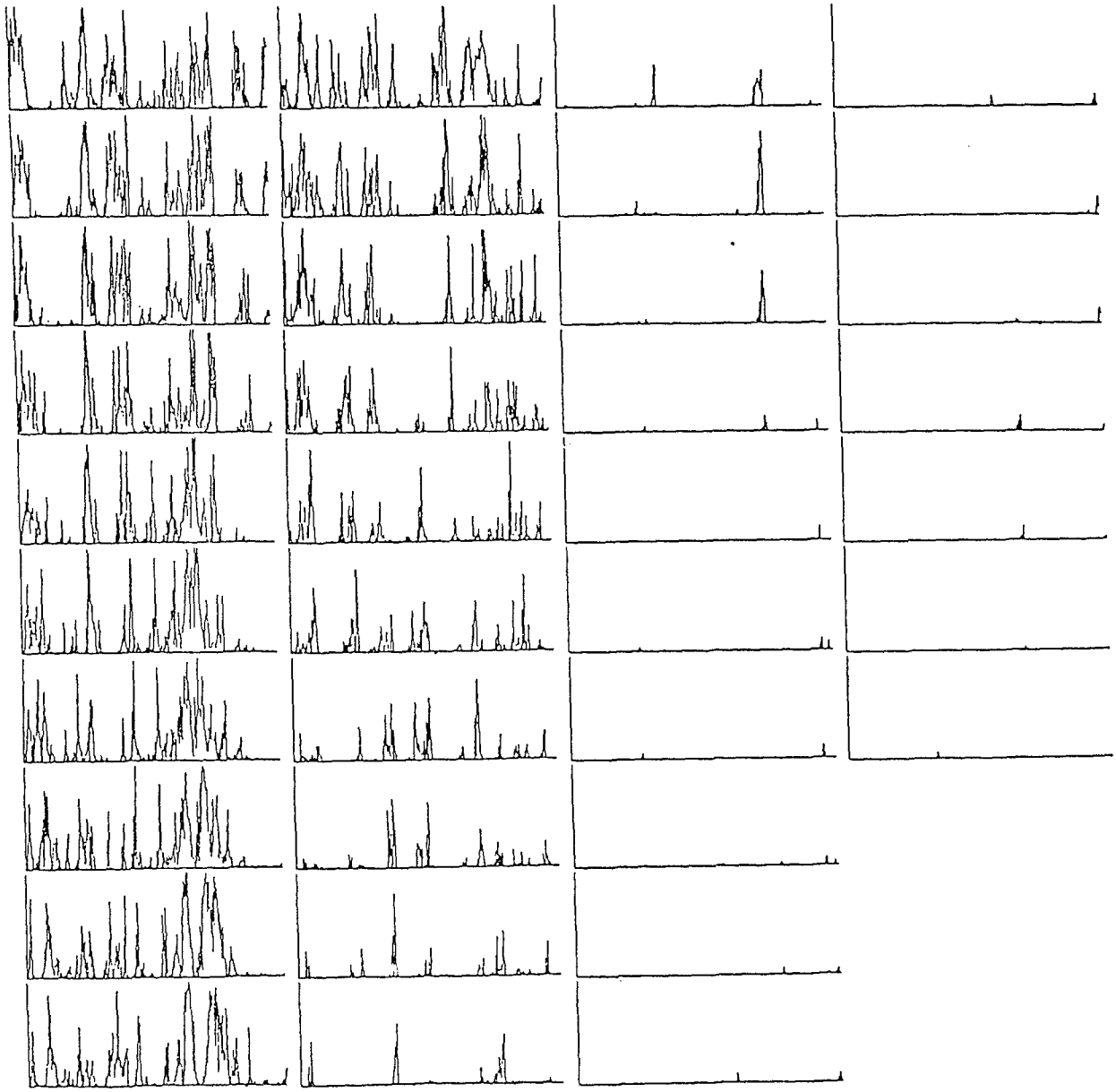

FIG. 1. Time series of GOES Precipitation Index (GPI) for 2.5° × 2.5° grid box along the latitude band between 12.5° and 15.0°S. From the top to bottom and left to right, each time series represents the GPI in a grid box centered 178.75°E to 86.25°W.

time series represents the GPI in a grid box centered from 178.75°E to 86.25°W. Each time series starts on 19 December 1987 for 100 days taken at 3-hour intervals, the abscissa represents the time, and the ordinate indicates the GPI from 0 to 1. The high fluctuations at the SPCZ region and dry southeastern Pacific are well demonstrated.

## 3. Analysis

First the mean and standard deviation of the GPI were calculated and are presented in Fig. 2. The major convective and dry regions are evident. Note the similarity of the two fields, which will lead to a simple relationship for the ratio (CV, the coefficient of variation) that will be referred to later. From Fig. 1 we conclude that estimation of the parameters in certain dry regions such as the southeastern Pacific is not meaningful because the aggregate rain is probably due to only a few events. Therefore, we restrict our analysis to only the areas with appreciable convective activity (mean above 0.025 and standard deviation above 0.05 on our GPI scale).

We do not attempt to present rainfall statistics from our GPI because of its uncertainty in representing ac-

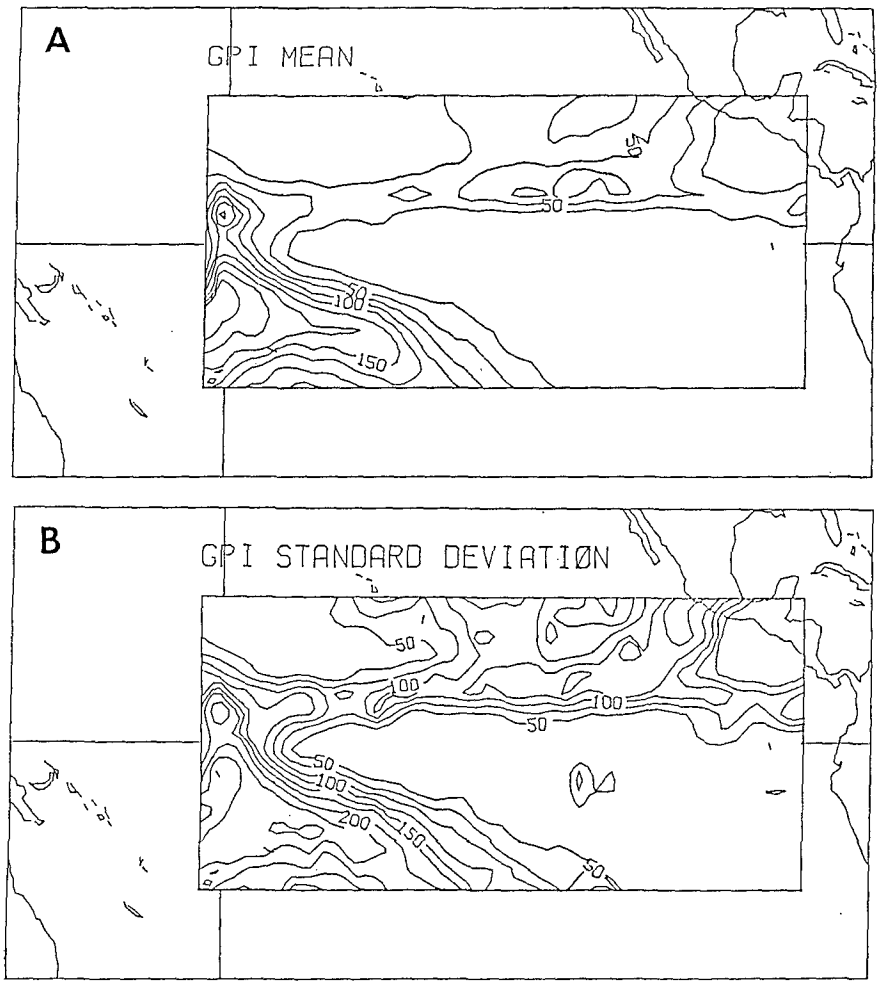


FIG. 2. The mean (a) and standard deviation (b) of the GPI. The contour scale is multiplied by 1000.

tual rainfall. [Our GPI is proportional to Arkin's GPI by a simple factor: rain rate is $R(\text{mm/h}) \approx 3 \times$ our GPI]. It should be mentioned that the estimation technique is based upon an empirical procedure possibly specific to the area and season of calibration. Although it has proved to be very useful, it must be regarded as an index until ways are found to extend the calibration over the global tropics.

We propose that the time series of area-averaged rainrate can be represented as the sum of a first-order Markov process (Laughlin 1981; Bell 1987) and a few sinusoids at discrete frequencies. Using the autocorrelation coefficient of lag 1 ($\alpha$), the autocorrelation time ($\tau_0$) can be estimated by $e^{-1} = \alpha^{\tau_0}$. The background red noise spectra are also calculated by the $\alpha$ values derived from the data. Then the power spectrum is calculated from autocovariances up to 32 lags based upon the GPI time series of 800 points at 3 h intervals. Variances at the diurnal and semidiurnal frequencies are estimated by subtracting the background red noise spectrum from the computed power spectrum. To estimate the peak times of the diurnal and semidiurnal cycles, pure sine series that have diurnal and semidiurnal cycles are generated. Then time lags are estimated from the phase spectrum through cross-spectral analysis. The peak times are adjusted to local time at each longitude. The "IMSL" subroutine "FTFREQ" was utilized for spectral estimations, and analyses were conducted on GPI25 and GPI50, separately.

Figure 3 illustrates an example of a normalized power spectrum of a GPI series, red noise spectrum as a background fluctuating component, and upper and lower 95% confidence limits at a grid box located in SPCZ. It shows a well-defined red noise spectrum, diurnal, and semidiurnal cycles of area-averaged rainrate. The confidence limits are calculated based on an assumed Gaussian distribution of rainrates. Since the rain distribution is non-Gaussian, the limits are not strictly valid, but should be useful as a guide. Note that in principle the diurnal cycle and its harmonics are

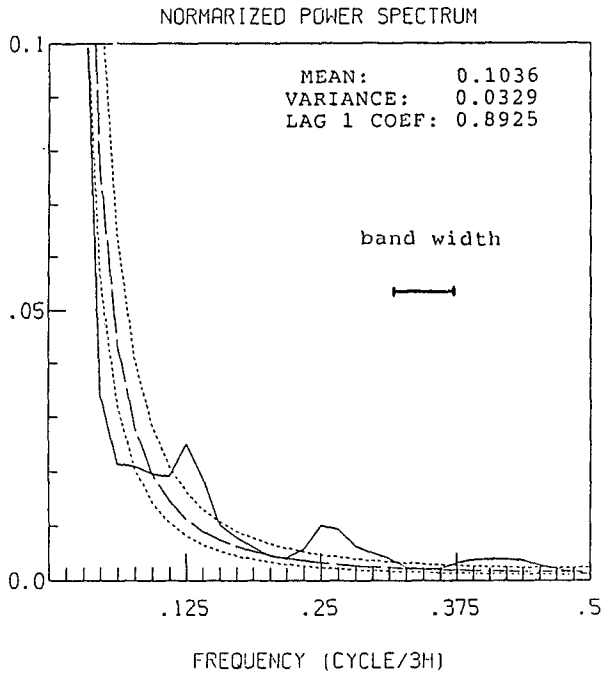


FIG. 3. The (normalized) power spectrum (solid), red noise spectrum (broken), and 95% confidence limits (dotted) of the GPI time series at the 2.5° × 2.5° grid box centered at (16.25°S, 143.75°W).

infinitely sharp, the widths in Fig. 3 are due to our own imposed bandwidth. Presumably, the area under the bumps should all be concentrated in the "spectral line."

## 4. Results

### *a. Coefficient of variation of area-averaged rain rate*

Figure 4 shows the relationship between the mean ($\mu$) and standard deviation ($\sigma$) of area-averaged rain rate at G25 and G50, respectively. The scatter diagrams show interesting relationships between the parameters, possibly quadratic relationships, in both grid sizes. To test whether these statistics were location-dependent, the scatter plots were differentiated by identifying three regions; however, we could not find any systematic dependence upon location. The CV at G50 is smaller than that at G25 as expected.

The relationships determined by a least-squares fit to a parabolic form between the parameters are also presented in Fig. 4c. These results indicate that the coefficient of variation ($\sigma/\mu$; CV) is not a constant, rather it depends upon area-averaged rain rate. As shown in Fig. 4c, the dependence is nearly quadratic, the linear term being only marginally significant in both cases. This finding is consistent with a simple Poisson process for the area-averaged rain rates. Consider the simple model for area-averaged rain rate, $R = xR_o$, where $R$ is the area-averaged rain rate, $x$ is a Poisson-distributed variate, and $R_o$ is the average rain rate when raining. The random variable $x$ may be thought of as the (small on the average) fraction of area in the averaging box where it is raining. This scheme has the property that $\mathrm{Var}(x) = \mathrm{Mean}(x)$, which leads to the quadratic dependence in Fig. 4. The Poisson model also suggests that the CV should fall by a factor of two when the area is quadrupled, as when going from the G25 to the G50 cells; this is also much larger than suggested by Fig. 4c. Hence, the Poisson model is an interesting guide but fails in some aspects of the description.

Laughlin (1981) showed that the CV in the GATE B-scale hexagon (about the same area as G25) was approximately 1.44 [=(0.711/0.492)] in Phase I and 1.27 [=(0.491/0.386)] in Phase II. Using the parabolic relation here we get 1.41 in Phase I and 1.13 in Phase II. Although some discrepancy is apparent for Phase II, we still find the value to be within the scatter of the diagram. Shin and North (1988) and Bell et al. (1989) used a value of CV near-unity for G50 in their sampling error studies for TRMM. The relation here suggests a

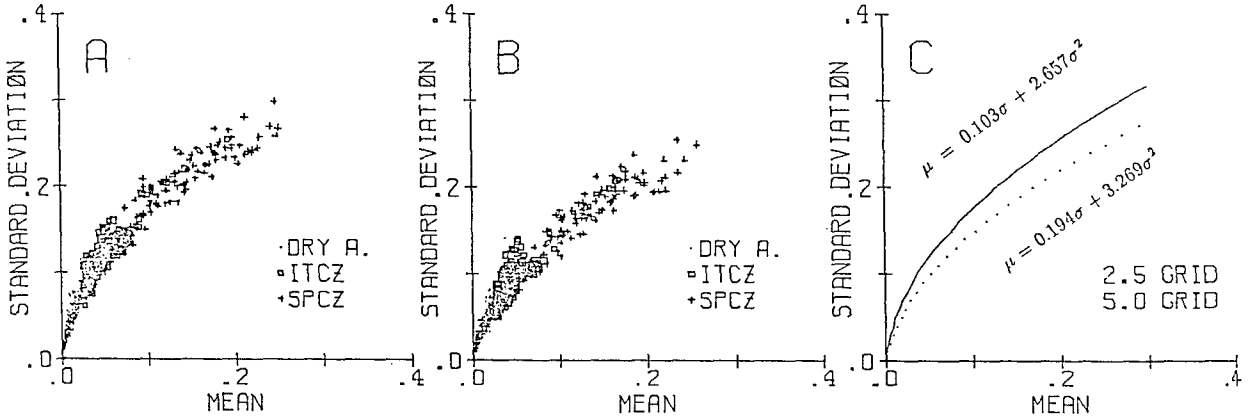


FIG. 4. Scatter diagram of the GPI mean vs standard deviation at each grid box of 2.5° × 2.5° area (a) and 5° × 5° area (b). The least squares fit is presented in panel (c). In (a) and (b) dots represent grid boxes from the dry areas (mean < 0.025 or standard deviation < 0.05), crosses from the SPCZ and squares are from the ITCZ.

CV in G50 to be 1.3 and 1.4, respectively for the two phases of GATE. These values lie between the band, limited by 1.0 and 1.5 as suggested by Shin and North in their extrapolation from G25 to G50 for GATE data.

### b. *Lagged autocorrelation time scale*

Figure 5 illustrates the dependence of lagged autocorrelation time scale ($\tau_0$) over the domain for the G25 (thin arrow) and for the G50 (thick arrow). The direction of the arrow represents the time (hour) from the north to clockwise as indicated at the upper-left corner. Because the center of a grid box is different for G25 and G50, four adjacent statistics ($\tau_0$) are averaged for G25 for simultaneous comparison with G50.

At any location, as expected, $\tau_0$ of G50 has a longer time scale than that of G25. For a small area, the time scale of area-averaged rainrate is determined by the duration that an area is swept across by a storm. Therefore, time scales increase with increasing averaging area. From the GATE rainfall data (Hudlow and Patterson 1979), Bell (1987) showed a power-law dependence of $\tau_0(L) = cL^{2/3}$ where $L$ is the size of the edge of the square averaging-area and $c$ is a constant for areas smaller than 250 × 250 km. Presumably, the value of $\tau_0$ approaches a limiting value for large $L$, since storms essentially spend all of their lifetimes within the box in this case.

Along the ITCZ, the time scale of G25 is about 12 hours and that of G50 is slightly longer, in general. The eastern part of SPCZ shows similar characteristics. In these regions the GPI mean is generally less than 0.1. This analysis suggests that rainfall characteristics in those regions are somewhat stationary. The regions north of ITCZ toward Mexico show a large difference of the time scale for G25 and G50; both autocorrelation times are generally longer than that in the ITCZ. This might possibly be due to propagating high cirrus clouds termed by McGuirk et al. (1987) as "moisture bursts." In the SPCZ region most convection exhibits much longer time scales than that in the ITCZ, and the time scale of G50 is much longer than that of G25.

Adler and Negri (1987) have pointed out that rain estimation from the GPI used here tends to underestimate the rainfall early in the convective life cycle and to overestimate the subsequent rainfall. Therefore, the GPI variations are probably more persistent than actual rain variations. Direct comparison of the autocorrelation times to the same statistics in the GATE area (about 8 hours for B-scale hexagon, Laughlin 1981) is not possible. However, we suggest that the Pacific ITCZ has a time scale that is at least comparable to that of the GATE region, but the SPCZ region has a significantly longer time scale. This finding suggests that convection in the ITCZ and SPCZ are driven by different mechanisms because of large time scale differences of the small and large averaging areas. However, we reiterate that quantitative comparison is impossible because of the uncertainty of our GPI as a measure of real rainfall. We have also not yet processed data for the opposite seasons.

### c. *Characteristics of diurnal and semidiurnal cycles*

Figure 6 shows the amplitude and phase of diurnal and semidiurnal cycles estimated from the GPI25 over

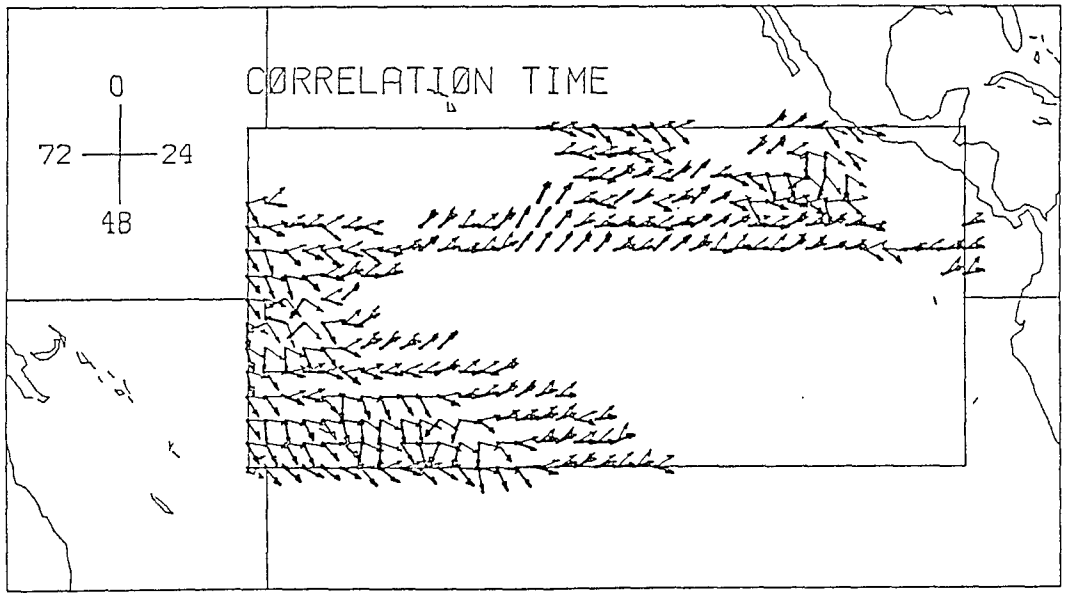


FIG. 5. Lagged autocorrelation time (hour) for 2.5° × 2.5° (thin arrow) and 5° × 5° (thick arrow) grid boxes. The direction of the arrow from the north to clockwise represents the autocorrelation time as indicated in the upper-left corner.

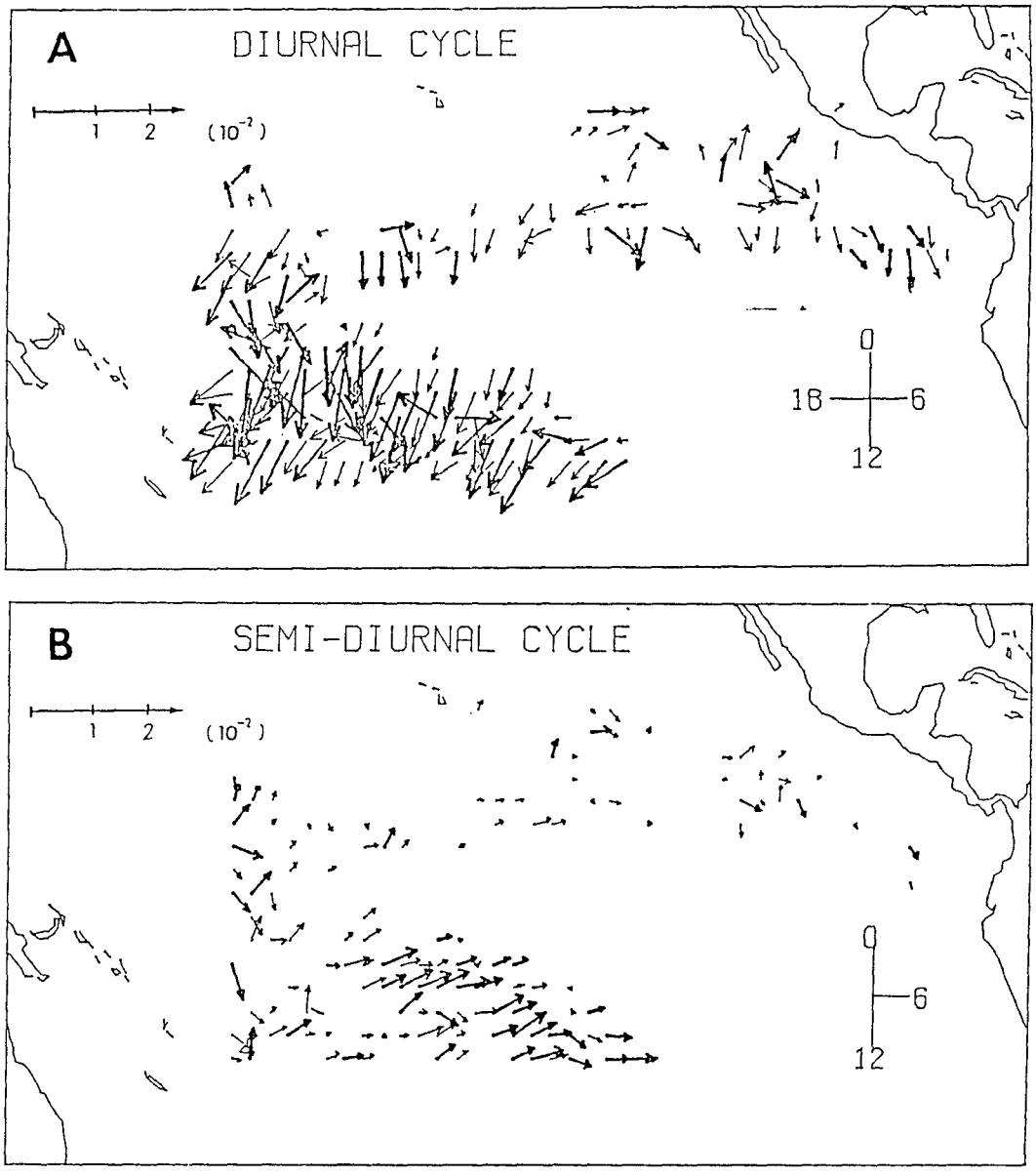


FIG. 6. The amplitude of the diurnal cycle (a) and semidiurnal cycle (b) of area-averaged rainrate for 2.5° × 2.5° grid box. The thin arrow indicates over 80% statistical significance and the thick arrow indicates those over 95% significance. The length is proportional to amplitude and the direction of the arrow indicates the time of maximum in a clock as shown in lower right-hand corner.

the domain. The length is proportional to the amplitude and the direction of the arrow indicates the local time of maximum in a 24 hour clock as shown in lower-right corner. The thin arrows indicate the amplitudes over 80% but less than 95% statistical significance, and the thick arrows indicate those over 95% significance with the assumption of Gaussian distribution as indicated earlier. Regions with less than 80% significance were not presented.

In the region of the Pacific ITCZ, the diurnal variations are basically composed of the first harmonic with a noon maximum, however, many of them are only marginally significant statistically. The semidiurnal cycle is weak in most of the ITCZ region. Regions north of ITCZ show midnight to dawn maxima of the first harmonics and small second harmonics. These results agree with Albright et al. (1985) in the regions of ITCZ and tropical intrusion region. Strong and statistically significant diurnal and semidiurnal cycles exist in the region of SPCZ. The maximum of the diurnal cycle occurs noon to midafternoon, however, phases of some regions in the SPCZ are incoherent. This may be due

to the propagating nature of rainfall in this region or simply sampling error. A similar report by Gruber and Chen (1988) of an analysis of OLR data from polar orbiters also indicates incoherent phases of the first harmonic over the SPCZ region. Significant semidiurnal cycles exist in the SPCZ and their maxima occur at dawn and midafternoon in this region generally (note two maxima of semidiurnal cycle). Therefore, the afternoon maximum is pronounced and the midnight minimum is depressed by the sum of the two harmonics. This agrees with the results of previous studies by Albright et al. (1985). One interesting thing is that a strong and significant second-harmonic exists in the relatively weak convective portion of the eastern SPCZ region. Strong convective regions show a relatively weak second-harmonic. Figure 7 shows the same analysis for G50. The features are more consistent but basically the same as those found in Fig. 6.

It should be noted that the intensity of the diurnal variation has traditionally been presented as its relative variation with respect to the mean. This may mislead in the absolute scale of their intensity. If the mean is small, a small variation of the diurnal scale is exaggerated and vice versa. We have chosen to present the diurnal variation in absolute scale in this study. The relative scale can be estimated by dividing the amplitudes by the mean as presented in Fig. 2.

The diurnal variation in the GATE region is com-

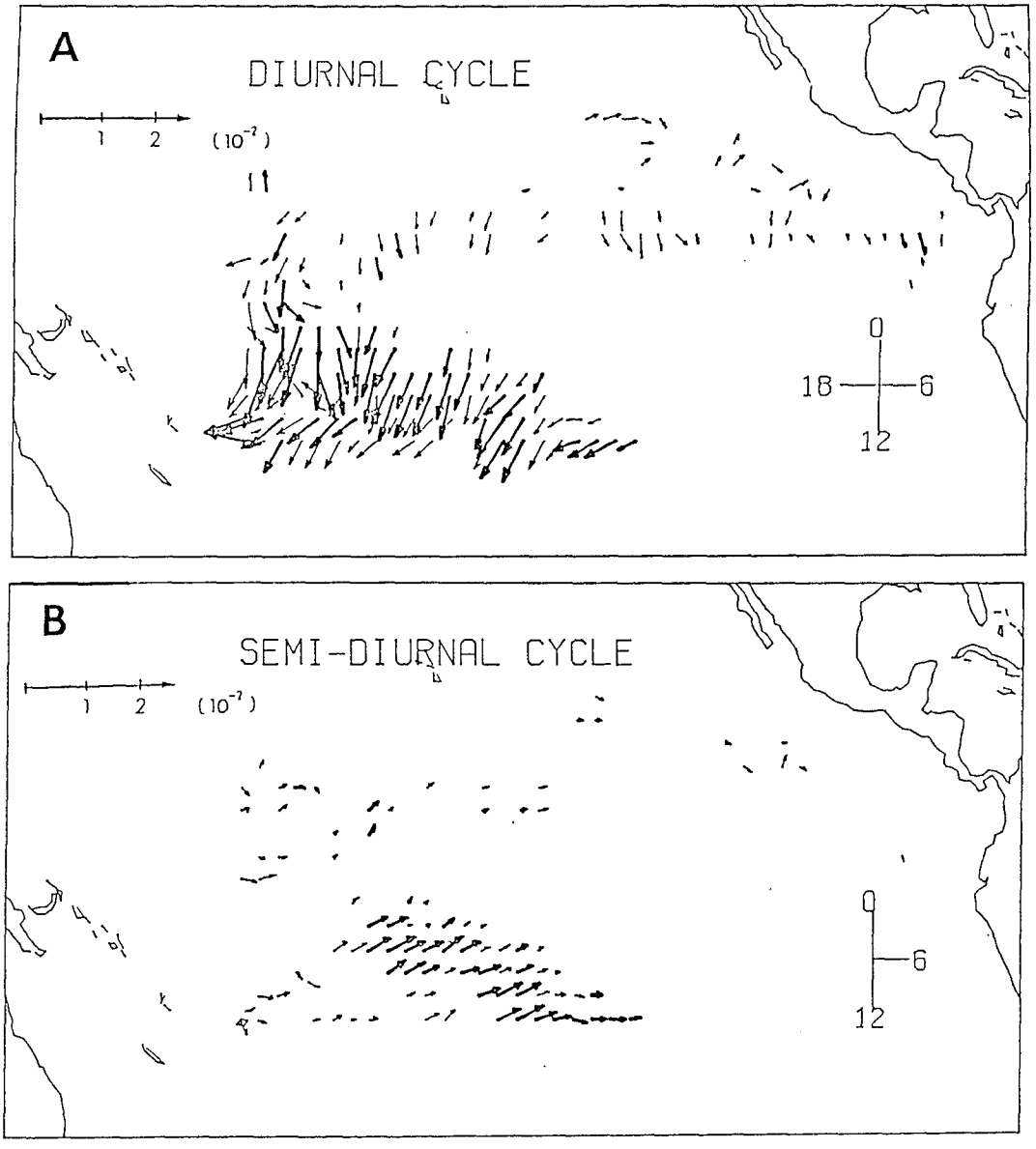


FIG. 7. Same as Fig. 6 except for a 5° × 5° grid box.

posed mostly of the first harmonic with a noon to mid-afternoon maximum that is similar to the Pacific ITCZ region (Albright et al. 1981). We suggest that the harmonic amplitudes of the diurnal variation of the Pacific and Atlantic ITCZ are similar and are composed mostly of the first harmonic. However, that of SPCZ appears to be different from the ITCZ with a stronger amplitude. We cannot claim with certainty that the results represent the climatic characteristics of convection over the tropical Pacific, since they may be different in other seasons or other years.

## 5. Conclusions

An investigation has been conducted to describe the characteristic time scales of area-averaged rainfall over tropical oceans in order to better understand the biases and random sampling errors to be expected for precipitation measurements from low-orbiting satellites that carry microwave radiometers. Due to the limited ability of our precipitation index to determine quantitative rainrates, we cannot give an unequivocal interpretation of the rainfall characteristics; however, we present the following tentative conclusions as possible guides for future mission design exercises.

The standard deviation of tropical oceanic rain bears a simple relation to the mean rain rate for area averages. This leads to the conclusion that the coefficient of variation can be characterized as a simple function of the mean. The functional form is suggestive of a Poisson process model. As expected the CV for smaller areas is larger than that for larger areas. The values of CV around the Pacific ITCZ are reasonably close to those observed in the GATE.

The time scales of area-averaged rainfall in tropical oceanic ITCZ regions are shorter than those in the SPCZ. The SPCZ regions show significant diurnal and semidiurnal cycles, but ITCZ regions show only a marginally significant diurnal cycle. The rainfall characteristics in the Pacific ITCZ appear similar to those in the Atlantic ITCZ in both time scale and diurnal variation. We must be careful to qualify some of our diurnal and semidiurnal cycle amplitudes since they may be season-dependent. For example, the present dataset is from the Southern Hemisphere summer and the nearly overhead sun may cause the excitation of the forced amplitudes to be larger than they might in the opposite season. Similarly, the ITCZ amplitudes may be stronger in near-equinox seasons since the sun is more nearly overhead during those times. We intend to explore those possibilities in future studies.

From the sun-synchronous satellite sampling point-of-view (return visits every 12 h to an averaging box), the existence of a fairly strong semidiurnal cycle over the SPCZ region adds an additional bias for precipitation measurements compared to the ITCZ. The longer red noise time scale in the SPCZ compared to that in the ITCZ actually reduces the purely random sampling errors due to the 12 h gaps between visits. Purely random sampling errors excluding the diurnal bias are expected to be about 10% (Shin and North 1988) for a sun-synchronous satellite based upon studies that made use of the parameters from GATE.

North and Nakamoto (1989) proposed a formalism for sampling error estimation in which the error can be derived by a product of a design-dependent filter (sampling strategy) multiplied by the space-time spectrum of the rain field. The sampling error for a large area can be written

$$\epsilon^2 = \int W(f)S(f)df$$

where $W(f)$ is a design dependent filter, $S(f)$ is the power spectrum of large area-averaged rainrates at a given frequency ($f$). For the satellite case, $W(f)$ is a series of spikes at the satellite visit frequency and its harmonics, hence the importance of the power at the semidiurnal cycle for 12 h recurring visits. For a very simple red noise model of the rain field (North and Nakamoto 1989) with a sinusoid added at the satellite revisit frequency, the formula reduces to

$$\epsilon^2 = \sigma_A^2 \frac{1}{\pi^2} \frac{\Delta t}{T} \frac{\Delta t}{\tau_0} + \Gamma^2$$

where $\sigma_A$ is the standard deviation of the area-averaged rain, $\tau_0$ is the autocorrelation time of the rain rate time series, $T$ is the long-term averaging interval (e.g., one month), $\Delta t$ is the interval between satellite visits and $\Gamma$ is the amplitude of the rain rate harmonic (if any) at the same frequency as the satellite revisits. The formula does not take account of partial visits of the satellite swath to the averaging box by assuming full-coverage visits at a fixed frequency. Our preliminary estimates, based for example on Fig. 3, indicate that the diurnal and semidiurnal cycles of the SPCZ might double the errors to be expected based upon pure red noise for a sun-synchronous satellite. Error enhancement due to diurnal effects in the ITCZ may be much smaller based upon the estimates of harmonic amplitudes in Fig. 7. It is interesting that the satellites such as TRMM (Simpson et al. 1988) whose orbits are inclined at 30° to 60° are "detuned" from the harmonics of the diurnal cycle and therefore are not modified by the $\Gamma^2$ term above. We expect to follow this work with a comprehensive examination of the errors to be expected for different satellite configurations.

*Acknowledgments.* The authors wish to thank D. Short, J. Newton, T. Bell and A. Gruber for numerous helpful discussions and comments. The work was partially supported by the Climate Analysis Center of NOAA, Grants NA87AA-D-CC118 and by the Climate and Radiation Office of NASA, Grant NAG5-868.

## REFERENCES


Adler, R. R., and A. J. Negri, 1987: A satellite infrared technique to estimate tropical convective and stratiform rainfall. *J. Climate Appl. Meteor.*, **26,** 1553–1564.

Albright, M. D., E. E. Recker and R. J. Reed, 1985: The diurnal variation of deep convection in the central tropical Pacific during January–February 1979. *Mon. Wea. Rev.*, **113,** 1163–1680.

——, D. R. Mock, E. E. Recker and R. J. Reed, 1981: A diagnostic study of the diurnal rainfall variation in the GATE B-scale area. *J. Atmos. Sci.*, **38,** 1429–1445.

Arkin, P. A., 1979: The relationship between fractional coverage of high cloud and rainfall accumulations during GATE over the B-scale array. *Mon. Wea. Rev.*, **107,** 1382–1387.

——, 1983: A diagnostic precipitation index from IR satellite satellite imagery. *Trop. Ocean-Atmos. Newsletter,* **17,** 5–7.

Bell, T. L., 1987: A space-time stochastic model of rainfall for satellite remote sensing studies. *J. Geophys. Res.*, **92,** 9631–9643.

——, A. Adbullah, R. L. Martin and G. North, 1989: Sampling errors for satellite-derived tropical rainfall: Monte Carlo study using a space–time stochastic model. *J. Geophys. Res.*, in press.

Gary, W. M., and R. W. Jacobson, Jr., 1977: Diurnal variation of deep cumulus convection. *Mon. Wea. Rev.*, **105,** 1171–1181.

Gruber, A., 1976: An estimate of the daily variation of cloudiness over the GATE A/B area. *Mon. Wea. Rev.*, **104,** 1036–1039.

——, and T. S. Chen, 1988: Diurnal variation of outgoing longwave radiation. *J. Climate,* **8,** 1–16.

Hudlow, M. D., and V. L. Patterson, 1979: GATE Radar Rainfall Atlas. NOAA Special Rep. [Available from U.S. Govt. Printing Office, Wash. DC, NTIS No. N80-21003.]

Laughlin, C. R., 1981: On the effect of temporal sampling on the observation of mean rainfall. *Precipitation Measurements from Space,* Atlas D., O. Thiele, Eds. [Available from NASA/GSFC, Greenbelt, MD.]

McConnell, A., and G. North, 1987: Sampling errors in satellite estimates of tropical rain. *J. Geophys. Res.*, **92,** 9567–9570.

McGarry, M. M., and R. J. Reed, 1978: Diurnal variations in convective activity and precipitation during Phase II and III of GATE. *Mon. Wea. Rev.*, **106,** 101–113.

McGuirk, J. P., A. H. Thompson and N. R. Smith, 1987: Moisture bursts over the tropical ocean. *Mon. Wea. Rev.*, **115,** 787–798.

Meisner, B., and P. A. Arkin, 1987: The relationship between large-scale convective rainfall and cold cloud over the western hemisphere during 1982–1984. *Mon. Wea. Rev.*, **115,** 51–74.

Murakami, M., 1979: Large-scale aspects of deep convective activity over the GATE area. *Mon. Wea. Rev.*, **107,** 994–1013.

North, G. R., 1987: Sampling studies for satellite estimation of rain. Preprints, *Tenth Conf. on Probability and Statistics in Atmospheric Science,* Edmonton, Amer. Meteor. Soc., 129–135.

——, and S. Nakamoto, 1989: Formalism for comparing rain estimation designs. *J. Atmos. Oceanic Technol.*, in press.

Reed, R. J., and K. D. Jaffe, 1981: Diurnal variation on summer convection over West Africa and the tropical eastern Atlantic during 1974 and 1978. *Mon. Wea. Rev.*, **109,** 2527–2534.

Richards, F., and P. Arkin, 1981: On the relationship between satellite-observed cloud cover and precipitation. *Mon. Wea. Rev.*, **109,** 1081–1093.

Shin, K.-S., and G. R. North, 1988: Sampling error study for rainfall estimate by satellite using a stochastic model. *J. Appl. Meteor.*, **27,** 1218–1231.

Simpson, J. R., R. Adler and G. North, 1988: A proposed tropical rainfall measuring mission (TRMM). *Bull. Amer. Meteor. Soc.*, **69,** 278–295.

Wexler, R., 1983: Relative frequency and diurnal variation of high cold clouds in the tropical Atlantic and Pacific. *Mon. Wea. Rev.*, **111,** 1300–1304.